Domer, B., Fest, E., Lalit, V. and Smith, I.F.C."Combining dynamic relaxation method with artificial neural networks to enhance simulation of tensegrity structures", J of Structural Engineering, Vol 129, No 5, 2003, pp 672-681. http://cedb.asce.org

Combining the Dynamic Relaxation Method with Artificial Neural Networks to Enhance the Simulation of Tensegrity Structures

Bernd Domer[1], Etienne Fest[2], Vikram Lalit[3], Ian F. C. Smith, M.ASCE[4]

Keywords: tensegrity, tension-structures, dynamic relaxation method, neural networks

Abstract

Structural analyses of tensegrity structures must account for geometrical non-linearity. The dynamic relaxation method correctly models static behavior in most situations. However, the requirements for precision increase when these structures are actively controlled. This paper describes the use of neural networks to improve the accuracy of the dynamic relaxation method in order to correspond more closely to data measured from a full-scale laboratory structure. An additional investigation evaluates training the network during service life for further increases in accuracy.

Tests showed that artificial neural networks increased model accuracy when used with the dynamic relaxation method. Replacing the dynamic relaxation method completely by a neural network did not provide satisfactory results. First tests involving training the neural network online showed potential to adapt the model to changes during service life of the structure.

1. Introduction

Cable structures, and tensegrity structures in particular, combine good load carrying capacity with low costs and aesthetics in unique ways. These qualities have been used to construct interesting structures, such as the Inland Revenue center in Nottingham (Wakefield 1999), the 2002 World Cup Main Stadium (Takenaka 2002) and the Georgia Dome (Geiger 2002). In extension to cable structures, tensile forces of tensegrities do not need to be anchored. They

[1] Res. Asst, Structural Engineering Institute, IMAC-IS-ENAC, 1015 Lausanne, EPFL, Switzerland
[2] Res. Asst, Structural Engineering Institute, IMAC-IS-ENAC, 1015 Lausanne, EPFL, Switzerland
[3] Software Eng., Geometric Software Solutions Co. Ltd., Bombay, India
[4] Prof. M. ASCE, Structural Engineering Institute, IMAC-IS-ENAC, 1015 Lausanne, EPFL, Switzerland, ian.smith@epfl.ch

are equilibrated by inner self-stress states. The most recent definition of tensegrity structures is given by Motro (2002):

> *"A tensegrity system is a structure in a stable, self equilibrated state that contains a discontinuous set of components in compression inside a network of components in tension."*

Tensegrity structures are complex. This is partly due to their geometrically non-linear behavior. Of all possible analysis methods for tensegrity structures, the dynamic relaxation method has proven to be the most advantageous in terms of speed and robustness. (Barnes 1977, Barnes 1994). Dynamic relaxation is an iterative method which employs finite differences to converge to a static equilibrium position. Since revised node positions are part of the results, the method is useful for form finding (Motro 1990) as well as for structural analysis (Wakefield 1999).

Additionally, it has been shown that simple structural principles, such as Maxwell's rule, cannot be applied to tensegrity systems (Calladine 1978). The composition and analysis of an equilibrium matrix, which links nodal loads to member forces (Pellegrino and Calladine 1986), provides deeper insights into the properties of such structures.

Recent proposals discuss building intelligent structures through combining active structural control with tensegrity systems (Smith and Shea 1999). To avoid control instabilities, the determination of control commands requires precise methods for predicting behavior. Experimental work has shown that the dynamic relaxation method simulates accurately the behavior of a full-size experimental structure in most cases (Fest et al. 2003). Nevertheless, inaccuracies have been found when comparing measurements with calculated deflections. Such inaccuracies lower the effectiveness of the dynamic relaxation method for computational structural control.

Material parameters have been determined through a testing program that was independent of the full-scale tests (Fest et al. 2003). However, some parameters such as node friction and cable relaxation are difficult to quantify. This paper includes a proposal for the use of a neural network as an intermediate error-correction step between structural analysis results using the dynamic relaxation method and the results used for the determination of control commands.

Artificial neural networks are useful for many applications in civil engineering (Garrett et al. 1997). They are a simplified description of the human brain as a structural metaphor. A relation between an n-dimensional input vector and an n-dimensional output vector is established according to training examples. They have been used in structural engineering to predict the deformations of beams that are strengthened by carbon fiber reinforced plastic sheets (Flood et al. 2000); to aid engineers during the conceptual stage of the design process (Rafiq et al. 2000); and for structural optimization (Kaveh and Iranmanesh 1998). Rehak and Garrett (1992) envisioned the use of neural networks in structural control, while Zagar and Delic (1993) have studied neural-network control of the deflection of a bridge by predicting actuator commands.

In contrast to these approaches, where neural nets are proposed to replace mechanical models or control formulations completely, this paper reports on a study of a combination of an established analysis method (dynamic relaxation) with a neural net. More specifically, the objectives are to:

- Review and verify the advantages of the dynamic relaxation method for the simulation of cable structures using a tensegrity structure as an example.
- Determine whether correcting dynamic relaxation results using neural networks leads to increases in accuracy.
- Train the neural network during service and quantify contributions to further increases in accuracy.

- Evaluate the potential for complete substitution of the dynamic relaxation method by a neural network.

2. Tensegrity structures

2.1 General remarks

Tensegrity structures consist only of compression (bars) and tension (cables) members, where cables surround bars. Buckminster Fuller has created the notion “Tensegrity” as a concatenation of the two words “tension” and “integrity” (Fuller 1962). The tension element provides the structure with a lightweight appearance. Therefore, Fuller characterizes these systems as “small islands of compression in a sea of tension”.

In contrast with cable structures, tensile forces in tensegrity structures are controlled by inner self-stress states (Motro 1992, Williamson and Skelton 1998). They are self-supporting and need no costly anchorages. Since they can be assembled and dismantled quickly, they are an attractive solution for temporary structures such as those used for fairs and expositions. When controlled actively, they have the added potential of becoming *part of* an exposition.

2.2 General properties of tensegrity structures

It has been shown by Calladine that Maxwell’s rule cannot be applied to determine whether a tensegrity system is stable (Calladine 1978). Pellegrino and Calladine showed that the equilibrium matrix **H** can be used to determine properties of tensegrity structures (Figure 1) (Pellegrino and Calladine, 1986).

The equilibrium matrix describes the relation between the nodal loads and the member forces and provides information about structural properties such as the number of independent self-stress states and mechanisms. A self-stress state describes a state where the structure is in equilibrium because of unilateral element forces. The number of independent stress states, s, of a cable structure can be determined using the following equation:

$$s = m - r\,, \tag{1}$$

where m = number of links (bars and cables) and r = rank(**H**)

Mechanisms have to be distinguished in two categories: infinitesimal and finite. Finite mechanisms allow node displacements without changing element-length. Infinitesimal mechanisms describe nodal displacements where changes in element lengths are of lower order than changes in nodal displacements. In general, tensegrities have infinitesimal mechanisms. The number of mechanisms, q, is calculated as follows:

$$q = n - r\,, \text{ with } n = 3 \cdot J\,, \tag{2}$$

where J = number of non-constrained joints.

Pellegrino and Calladine (1986) showed further that the compatibility matrix **C**, which links nodal displacements and bar elongations, can be obtained simply by transposing the equilibrium matrix:

$$C = H^T \tag{3}$$

These expressions will be used in Section 3 to evaluate the properties of a full-scale tensegrity module.

In contrast with traditional structures composed of rigid materials, the shape of a tensegrity structure is not known in advance. Before initiating a formal structural analysis, a form finding step is necessary. This step, which consists in a search for the minimum surface between fixed points or borders, may be performed experimentally. For example soap films have also been used for experimental form-finding (Figure 2) (Bach et. al. 1988). The surface tension of the soap film creates the smallest possible surface between fixed borders. Nevertheless, most form-finding tasks are performed analytically; this research employs the dynamic relaxation method, as described in Section 2.3.3.

After form-finding, forces and displacements of the tensegrity structure are calculated. Since this type of structure behaves non-linearly, equilibrium conditions cannot be formulated on the undeformed system. For simple systems, such as a cable between two supports (Figure 3), an analytical solution is available. The system becomes stiffened only when it is deformed. For this case, the following expression relates loading and prestress (Scharpf 1981) (see Figure 4):

$$P = \frac{2w}{\sqrt{l_0^2 + w^2}} \left[N_0 + \frac{EA}{l_0} \left(\sqrt{l_0^2 + w^2} - l_0 \right) \right] \tag{4}$$

2.3 Simulation of tensegrity structures

2.3.1 Form-Finding with the force density method

The force density method has been proposed by Schek to determine possible shapes of equilibrium of a pin-jointed network consisting of cables and bars (Schek 1973). It is stated that any state of equilibrium of a net structure can be obtained by solving a system of linear equations.

The ratio between the branch forces and the branch lengths of the network is called force density. Given loading, support conditions and force densities, shapes of cable structures can be determined. Schek has also extended this method for other situations such as fixed force densities.

2.3.2 Matrix and vector methods

Analytical methods for the simulation of cable structures such as tensegrity systems are classified as follows (Barnes 1977):

- Incremental methods
- Iterative methods

- Minimization methods

Incremental and iterative methods use the matrix formulation of finite elements. The approach consists in solving a system of equations which links the stiffness matrix *K* with the vector of loads *P* to obtain the structural deformations δ (Szilard 1982) (Equation (5)):

$$P = K \cdot \delta \tag{5}$$

Non-linear behavior may be taken into account through adding the $\mathbf{K^{NL}}$ stiffness matrix to the linear stiffness matrix **K**. The incremental Euler-method solves this system of equations by applying the load, ΔP, stepwise. The stiffness-matrix $\mathbf{K^{L}} + \mathbf{K^{NL}}$ is iteratively re-assembled to correct for deformations:

$$\Delta P = \left(K^{L} + K^{NL}\right) \cdot \Delta\delta \tag{6}$$

Iterative methods, such as the Newton/Raphston method also employ Equation (6). However, instead of applying the load stepwise, the residual forces at the nodes are minimized during iterations.

Although matrix-methods generally require fewer iterations than minimization methods, non-singular stiffness matrices are necessary. As a vector-based method, the dynamic relaxation method does not require such complexity. The dynamic relaxation method decouples equilibrium and compatibility until convergence to an equilibrium position is achieved. All methods include conditions in order to assure convergence. Since the stiffness relationships are represented separately, vector techniques are easier to accomodate (Wakefield 1999).

2.3.3 Structural analysis with the dynamic relaxation method

The dynamic relaxation method is widely used for static structural analyses of cable structures. The method uses the dynamic equation of a damped system with an externally applied load to calculate the static behavior of structures (Barnes 1977, Underwood 1983):

$$P(t) = M\ddot{d} + C\dot{d} + Kd \tag{7}$$

The motion of the structural nodes is traced over time until the sum of residual forces in the nodes converges to a near '0' value. This indicates that the state of equilibrium of the structure has been reached. The residual forces $R^t_{i;(x,y,z)}$ in each node *i* can be calculated by

$$R^t_{i;(x,y,z)} = M_{i;(x,y,z)} \cdot \dot{V}^t_{i;(x,y,z)} + C_{i;(x,y,z)} \cdot V^t_{i;(x,y,z)}, \tag{8}$$

where V = vector of nodal velocities.

Parameters to be set are the fictitous masses, m, and fictitious damping, c, that are represented in the matrices **M** and **C** of Equation (7) as well as the time step Δt. Papadrakakis (1981) has compared several strategies for choosing these parameters in order to achieve rapid convergence. One of these strategies, kinetic damping, does not require determination of the viscous damping matrix C in Equation (8). The kinetic energy of the undamped structure is calculated, and whenever a kinetic peak is detected by a sudden fall of kinetic energy, the iteration steps back to the moment in time where the kinetic peak is assumed to have occurred. At this point, nodal velocities are reset to '0' and the current coordinates are taken as starting values for the next cycle of iterations. The strut element that was included in this analysis does not simulate buckling. Calculated compressive forces are checked against ultimate forces obtained by independent buckling tests.

If necessary, material non-linearity can be introduced at each time step, since no pre-assembled stiffness matrix is used. Whenever a cable receives a compressive force during one time step, its inner force is set to 0 for the subsequent step. Because the dynamic relaxation method calculates nodal displacements when calculating the member forces, a separate form-finding process is not necessary.

3. Tensegrity structure

3.1 Description of the tensegrity structure

A tensegrity structure has been constructed at the Swiss Federal Institute of Technology (EPFL) to perform research in the field of active structures (Figure 5). It consists of three modules. Each module includes the central node, where the three bars forming the upper pyramid are joined to the three bars forming the lower pyramid. Twenty-four stainless steel cables connect the twelve joints of each module. Bars are made of fiber reinforced polyester tubes in order to examine a new application for this material and to facilitate measurement of deformations.

Analysis control software (TSACS) has been developed. It uses the dynamic relaxation method (Rossier, personal communication, 1994) to calculate forces and displacements of the system and provides graphical user interfaces for input and for results (Figure 6).

According to Calladine, this tensegrity module fails the stability test when analyzed using Maxwell's rule (Calladine 1978). The rule states that

$$3 \cdot j - 6 \tag{9}$$

bars are needed for structural stability, where j = number of joints assuming a statically determinate structure in three dimensions. Applying this to one module, we calculate that

$$3 \cdot 13 - 6 = 33$$

bars are needed to obtain static stability with Maxwell's rule. In these modules 30 bars and 13 joints provide static stability.

Assembling the equilibrium matrix **H** results in a rank of 27. Thus, the number of independent self-stress states is calculated using Equation (1):

$$s = m - r = 30 - 27 = 3$$

The number of mechanisms for one module is calculated using Equation (2):

$$q = n - r = 3 \cdot J - r = 30 - 27 = 3.$$

Since J is the number of non constrained joints. Initial prestress is applied to the structure when the telescopic bars are extended from their initial position. The notion of "2 mm prestress" means that all the bars have been uniformly extended by 2 mm more than their nominal initial length. Of several possible control objectives, maintaining the upper layer of the structure at a constant slope has been chosen as an initial research task (Figure 7). The slope is controlled by measuring the displacements of three nodes on the upper layer (nodes 6, 52 and 62 in Figure 7) and adjusting the telescopic bars such that they counteract displacements.

3.2 Coupling the dynamic relaxation method with neural networks

Perelli has shown that the dynamic relaxation method can be used to model this tensegrity structure (Perelli, personal communication, April 2000). Input parameters for the calculation have been determined according to the materials used through independent testing (Etienne Fest, personal communication, November 1999). A discrepancy between theoretical calculations and measured behavior has been observed. Although this might be acceptable for isolated calculations, errors may accumulate throughout a sequence of control commands under active control.

Node friction, cable relaxation, node deformation and changing environmental conditions are possible causes for differences between measured and predicted behavior. Values of these parameters are difficult to determine accurately (Fest et al. 2003). The next section discusses the potential for neural networks to increase the accuracy of the dynamic relaxation method since they are able to model non-linear relationships and are known to be efficient when applied to time-variant systems (Garrett 1997).

4. Neural networks

4.1 Description

Artificial neural networks establish relationships between m-dimensional input vectors and n-dimensional output vectors. Such relationships are particularly useful when no mathematical formulation is available. The core component of a neural net is the neuron or node. Nodes are used to connect the input layer, hidden layers and the output layer.

The nodes of hidden layers and the output layer receive input from the previous layer (α_i in formula 10). This input is multiplied by the weight, $w_{i,j,}$ of each internodal connection and summed up. The total activation of the node , x_j, is then calculated by subtracting the internal threshold, $T_{j,}$ from this sum (10).

$$x_j = \Sigma w_{i,j} \cdot \alpha_i - T_j \tag{10}$$

x_j is passed to the transfer function of the node ,F , which determines the final output, o_j.

For transfer functions (for a neural net's continuous and monotonic functions), the sigmoid function is chosen (11).

$$f(x) = \frac{1}{1+e^{-x}} \tag{11}$$

During the training phase, sets of known input/output patterns are processed. The weights of the internodal connections are adjusted to match the desired output.

Adjustments may be made by propagating back the error that is calculated as the difference between the output layer and the desired output. The factor that governs the amount of change in each node of the network during the backpropagation is called the learning rate (η_j). Since the sigmoid function is insensitive to input-values greater than two, the input vector should be normalized to an interval of [0,1]. For a more detailed description of neural networks refer to Pfeiffer and Scheier (1999) and Rojas (1996).

4.2 Stuttgart Neural Net Simulator (SNNS)

A wide choice of software exists for creating and testing neural networks. A particularly useful tool is the Stuttgart Neural Net Simulator (SNNS 2001). A graphical user interface helps design the network and offers a choice of learning methods and activation functions.

For more sophisticated tasks, a batch language may be used. The batch processor “batchman” processes small programs. Within the scope of this project, the graphical interface of SNNS has been used to create network topologies. “batchman” was employed for training and testing the networks.

5. Tests

5.1 Test description

The primary focus in testing was to determine whether using a neural network can increase the accuracy of the dynamic relaxation method when used alone (Perelli, personal communication, April 2000). Previous tests measured the displacement of three nodes on the upper layer of the structure. Ninety pattern sets consist of displacements calculated using the dynamic relaxation method and three measured displacements. Magnitudes and locations of the loading that lead to these pattern sets are presented in Table 1 and Figure 8. Load cases are subdivided into three classes that are named as follows: symmetric, asymmetric and central joint loading. Symmetric loading applies the same load magnitude to nodes whose combined center of gravity corresponds to the center of gravity of the structure. Asymmetric loading involves one edge node at a time and central joint loading means that the central joints of each module are loaded. Since the neural network is ultimately intended to be used for active control, results from a range of prestress levels were employed. Measurements were taken three times to exclude errors. This results in a total number of 270 pattern sets.

As described in Section 3.1, three nodes on the upper layer were used as reference points for slope control. Therefore, the goal of this work was to increase the accuracy of calculating

deflections at these three nodes. This goal thus fixed the number of input and the number of output nodes of candidate networks to three each. The number of nodes in the hidden layer was evaluated initially for twelve network topologies having zero, one and two hidden layers. The results of these tests indicated that four topologies had potential, and they were subsequently employed for the main testing phase. These topologies were

- 3-8-3
- 3-12-3
- 3-10-10-3
- 3-14-14-3

where first and last numbers indicate numbers of nodes in the input and output layer (three in every case). Numbers between the first and last numbers provide the number of nodes in the hidden layers. All networks being used were feed forward and used the sigmoid transfer function. The learning rate was set to $\eta = 0.2$.

Throughout all tests, pattern sets were subdivided into training, testing and unseen patterns. As their name indicates, training patterns were used to train the network. The weights of the network were changed after each training cycle to minimize the training error. After every 100 training cycles, the test patterns were presented to the trained network, and the test error was evaluated. Weights were only saved when the testing error decreased. It was observed that training errors decreased continually but test errors started to increase after some time. This is due to the fact that neural networks may over correlate training patterns when they have been subjected to too many training cycles. Unseen patterns were used after training and testing of the network to check overall generality.

A batch program was written using the Stuttgart Neural Net Simulator (SNNS) batch interpreter for training and testing the four network topologies. One-layer networks were trained for at most 500,000 cycles and the two layer networks for up to 1,500,000 cycles.

The error used is the sum of square error (SSE), which is equal to the sum of the square of the difference between normalized simulated and normalized targeted values.

In addition to primarily focusing on determining potential accuracy enhancement, two other applications of neural networks have been tested:

1. Examining the possibilities of online-training to adapt the neural net to changing loads and environmental conditions.
2. Compare correcting the dynamic relaxation method results with complete replacement by a neural network.

5.2 Enhancing the Accuracy of the Dynamic Relaxation Method

5.2.1 Using measured results

A total number of 270 patterns were available. The usual experimental procedure of eliminating unrealistic data resulted in the deletion of 30 patterns. The remaining 240 have been subdivided into three groups as follows:

- Training patterns: 150
- Test patterns: 39
- Unseen patterns: 17

Training of the four network topologies and subsequent testing reveals test errors that are given in Table 2. Finally unseen patterns are tested against tripled targeted values allowing 17 comparisons. This has been carried for the 3-12-3 and the 3-14-14-3 topology and results are shown in Figure 9. In this figure, deviations of simulated values from the targeted measured values are compared by calculating ratios of results when using neural networks (DR+NN) for an additional error correction step and when using only the dynamic relaxation method (DR) for simulation.

Values above the “1” axis represent, therefore, an increase; values below “1” represent a decrease in accuracy when using a neural network.

The best network (3-12-3) only increases accuracy in 3 out of 17 cases (13,15,16). In all other cases, there are losses in accuracy. It can be concluded that training the networks with these data sets does not contribute to the overall accuracy of the simulation. This observation also is clear when values of the average increase in accuracy are calculated (continuous and dotted lines in Figure 9) since they are less than one.

5.2.2 Using the average of the measured values

Since the initial choice of the training and testing patterns did not give encouraging results, and since each load case was tested three times, averages of these three test results were calculated.

This resulted in a total of 80 patterns and these were subdivided into 50 training, 13 test and 17 unseen patterns. The evaluation of the four network topologies identified the 3-8-3 and the 3-10-10-3 networks (Table 3).

Using the same schema as in Figure 9 to present the results, Figure 10 shows the evaluation of the unseen patterns. The situation has changed drastically: now there is only one data set out of 17 (in the 3-10-10-3 configuration) which shows a decrease in accuracy. The decrease of accuracy (15.75%) is a tolerable value, which is not expected to affect the stability of the structure in practice.

Figure 11 is a plot of the ratio of improvements of accuracy in Figure 10 for each unseen pattern. Values above the "1" axis indicate cases where the two layer network performed better than the one hidden layer network. The two hidden layer network is more advantageous than the one hidden layer network.

5.2.3 Using Jenkin's hypercube for the selection of training data

Results in Figures 9 and 10 demonstrate that training data characteristics affect the ability of the net to generalize. If too little data is used, the network will not be able to give a reasonable approximation. On the other hand, if too much data is presented, the network could model "too closely" this data (over conditioning); thus, it would not be able to generalize to other data.

Modeling relationships beyond the scope of the training patterns is difficult for statistical methods such as neural networks. Therefore, input-output training patterns should contain data that correspond to even distributions between the borders of spaces of possible values.

Jenkin's hypercube concept evaluates data to determine whether the solution space is covered to the greatest possible extent (Jenkins 1997). The minimal number of training data needed depends on the number of output nodes. For example, three output nodes demand for a three-dimensional hypercube. A 3D-cube can easily be visualized and consists of 27 significant points since there are corners, mid-sides, mid-faces and a center (Figure 12). Unfortunately, the measurement data that is available in this study does not coincide with the optimal distribution described by Jenkin's hypercube. This is understandable since results are determined by specific loading configurations and the physical principles of structural behavior.

Although its main focus is to indicate the best distribution of training patterns, the model can be used to reduce the number of pattern sets needed for training. The focus of this test was to determine the potential for further reductions in the number of training patterns needed.

Therefore, two different testing and training pattern sets have been created: one by considering the hypercube concept (patternset “A”), the other by randomly choosing patterns (patternset “B”). The minimal number of 27 patterns has been used in both cases. The 3-8-3 and 3-10-10-3 network configurations have been trained with patternset “A” as well as with patternset “B”. All networks have been tested using the same unseen patterns as in Section 5.1. Accuracy decreased to unacceptable values in both cases.

5.3 Online Training

Online training enables modification of neural nets when environmental conditions change. Active tensegrity structures in practical situations could use such functionality. Online training consists of, first, adding new measurements taken during service life of the structure to the training data and, second, retraining the network. Since computational time can be excessively long during service, the training time needed for the network becomes an important issue.

In an initial study, the most promising network topologies from Section 5.2 were chosen: the one layer (3-8-3) configuration and the two-layer configuration (3-10-10-3). The networks that have already been trained with 19 pattern sets have been trained for three further cycles. In each cycle, one pattern set has been added to the training data. This results in a total number of 20, 21 and 22 patterns for the first, second and third set. The network is then trained until the test error starts increasing and are than trained for 10 further seconds. The error decreased by 1.9 % for the 3-8-3 configuration and by 0.55 % for the 3-10-10-3 configuration. These decreases are not large enough to warrant such functionality at this time. Further work is required to determine the characteristics of the most useful training sets.

5.4 Substituting the dynamic relaxation method completely with artificial neural networks

The present model uses the dynamic relaxation method in combination with a neural network to calculate the nodal displacements of the tensegrity structure. It could be argued that one neural network might be able to replace the dynamic relaxation method completely. This would save much computational time. As a first step, it was checked whether the dynamic relaxation method could be replaced by a neural network. This has been tested using data taken from analysis results.

When all 33 nodes of the three-module structure are modeled, an extremely complex network follows. Complexity increases exponentially with the addition of modules.

Test data were generated analytically for a network where the dead load was constant and the structure was loaded at one point. Starting with three nodes in the input layer and one node in the output layer, the network has been trained for 60,000 epochs. A 3-8-8-1 configuration has been used. Although a sufficiently low training error was attained, the test patterns are further away from the desired output (Figure 13).

Until now, the sigmoid function has been used as an activation function with normalized values between [0;1]. The tan hyperbolic function has been chosen to enlarge the bandwidth and normalization between –1 and +1; therefore, allowing a more precise normalization. More training patterns than used in previous tests have been generated. As Figure 14 shows, the deviations increased dramatically. Further tests have been performed using another method of normalizing input data as well as with other network topologies (3-8-8-3 and 3-12-12-3). None revealed satisfactory results.

6. Discussion and Conclusions

Artificial neural nets provide a useful complement to simulation using the dynamic relaxation method. Even when used with sparse training data, they lead to increased model precision while maintaining explicit structural knowledge. Such a combination is clearly better than the use of neural nets alone. Other types of neural networks exist and might show advantages over the one used. Additional training patterns are needed for further decreases of the overall error. The measurement data, which has been used for the training of the neural network, is related to the configuration of the structure. Future work involves studying to what extent the neural network can be used to correct analysis of structure with more than three modules, different geometries and materials.

In exceptional cases where the neural net is not able to increase accuracy, its use is not expected to affect the reliability of the model for iterative active control.

Although the strategy of selecting training data according to a hypercube configuration has been used successfully for other applications, its implementation is complicated by distribution characteristics of the measurement data. A hypercube distribution might, nevertheless, prove to be a useful filtering strategy when the structure is controlled actively, since large numbers of measurements will become available.

Online training may be useful for further increasing the precision of the model and for adapting the neural net to changing environmental conditions. Although the improvement of 1.9 % does not yet justify implementation, there is potential for further enhancements. This functionality requires further investigation. The following issues are examples of important aspects:

- Evaluation of the quality of the training pattern proposed by the measurement system
- Deletion of old pattern sets without affecting accuracy

These aspects are similar to concepts of case-based reasoning and case maintenance (Smyth and Keane 1995).

Several network configurations using various activation functions and methods for normalization of input values have been studied -- no justification for complete replacement of the dynamic relaxation method with a neural network could be found.

The principle conclusions of this study are as follows:

1) Neural networks enhance the accuracy of the simulation of tensegrity structures
2) Replacing dynamic relaxation with a neural networks is not justified
3) Although online training has potential, further work is needed to justify use

This study provides important contributions to the implementation of actively controlled tensegrity structures.

7. Acknowledgements

This research is partially funded by the Swiss National Science Foundation No. 2000-061756. We grateful acknowledge the suggestions of Ashok Gupta (IIT Delhi), which led to test whether the dynamic relaxation method can be completely replaced by neural networks. We would like to thank Dr. Alan Kwan, Cardiff University of Engineering, Dr. Benny Raphael for discussions and Yann Perelli for performing some of the experiments.

8. Notation

The following symbols are used in this paper:

A	=	area
C	=	damping matrix
d	=	vector of nodal displacements
E	=	module of elasticity
H	=	equilibrium matrix of cable structures
J	=	number of non-constrained joints
K, K^l	=	stiffness matrix
$\mathbf{K^{NL}}$	=	non-linear stiffness matrix
M	=	mass matrix
P	=	single load
P(t)	=	vector of nodal forces, varying with time
R	=	vector of residual forces
q	=	number of mechanisms
r	=	rank of equilibrium matrix **H**
m	=	number of links (bars and cables) of cable structures
s	=	stress states of cable structures
V	=	vector of nodal velocities
w	=	deflection
δ	=	deformation

9. References

Bach, K., Burkhardt, B., Otto, F. (1988). “Seifenblasen-Forming Bubbles, IL 18“, Universität Suttgart, Institut für leichte Flächentragwerke, Karl Krämer Verlag, Stuttgart.

Barnes, M. R. (1994). “Form and stress engineering of tension structures”, *Structural Engineering Review*, 6(3-4), pp. 175-202.

Barnes, M. R. (1977). “Form Finding and Analysis of Tension Space Structures by Dynamic Relaxation”, PhD-Thesis, The City University of London.

Calladine, C. R. (1978). “Buckminster Fuller's "Tensegrity" Structures and Clerk Maxwell's Rules for the Construction of Stiff Fames”, *Int. J. Solids Structures*, Vol. 14, pp. 161-172.

Fuller, B. (1962). “Tensile Integrity Structures”, U.S. Pat. 3,063,521.

Fest, E., Shea, K., Domer, B., Smith, I. F. C. (2003): “Adjustable tensegrity structures”, *ASCE Journal of Structural Engineering*, in press.

Flood, I., Nandy, S., Muscynski, L. (2000). “Assessing External Reinforcement on RC Beams Using Neural Nets”, *Proceedings of: Computing in Civil and Building Engineering, ICCCBE-VIII*, August 14.-16., Stanford, CA ASCE Publication, pp. 1114-1120.

Geiger (2002). “Tensile Membrane Projects”, http://www.geigerengineers.com, last visited May 2002.

Garrett, J. H. Jr., Gunaratnam, D. J., Ivezic, N. (1997) “Introduction”, Kartam, N., Flood, I., Garrett, J. H. Jr. (eds.): *Artificial Neural Networks for Civil Engineers: Fundamentals and Applications*, ASCE Publication, pp. 1-18.

Jenkins, W. M. (1997). “Approximate analysis of structural grillages using a neural network”, *Proceedings ICE, Structs. & Buildings 122*, pp. 355-363.

Kaveh, A., Iranmanesh, A. (1998). “Comparative Study of Backpropagation and Improved Counterpropagation Neural Nets in Stuctural Analysis and Optimization”, *International Journal of Space Structures*, 13(4), pp. 177-185.

Motro, R. (2002). “Tensegrity: the state of the art”, *Proceedings of Space Structures 5*, University of Surrey, Guildforth, Thomas Telford publishing, pp. 97-106.

Motro, R. (1992). “Tensegrity Systems: The State of the Art”, *International Journal of Space Structures*, 7(2), pp. 75-83.

Motro, R. (1990) Tensegrity Systems and Geodesic Domes, *International Journal of Space Structures*, 5(3-4), pp. 341-351.

Papadrakakis, M. (1981). “A Method for the automatic evaluation of dynamic relaxation parameters”, *Computer Methods in Applied Mechanics and Engineering*, 25, North-Holland Publishing Company, pp. 35-48.

Pellegrino, S., Calladine, C.R. (1986). “Matrix Analysis of Statically and Kinematically Indeterminate Frameworks”, *International Journal of Solids and Structures*, 22,(4), Pergamon, pp. 409-428.

Pfeiffer R., Scheier C. (1999). “Neural Networks for Adaptive Behavior”, *Understanding intelligence*, MIT Press, Cambridge, Massachusetts, pp. 139-177.

Rafiq, M. Y., Bugmann, G., Easterbrook, D. J. (2000). “Artificial neural networks to aid conceptual design”, *The Structural Engineer*, 78(3), pp. 25-32.

Rehak, D. R., Garrett, J. H. Jr. (1992). “Neural Computing for Intelligent Structural Systems”, *Intelligent Structures 2*, Wen, Y. K, ed., Elsevier science, pp. 147-161.

Rojas, R. (1996). “Neural Networks - A Systematic Introduction”, Springer Verlag, Heidelberg.

Scharpf, D. (1981). “Zur Berechnung von Seiltragwerken“, *Berichtsband zur Vortragsveranstaltung Seile und Bündel im Bauwesen*, Beratungsstelle für Stahlverwendung, Düsseldorf, III.1-1 – 13.

Schek, H. J. (1973). “The Force Density Method for Form Finding and Computation of General Networks”, *Computer Methods in Applied Mechanics and Engineering 3*, North-Holland Publishing Company, pp. 115-134.

Smith, I. F. C., Shea, K. (1999): “Extended Active Control to Build Intelligent Structures”, *Proceedings, Structures for the Future - The Search for Quality*, IABSE Reports, Vol. 83, International Association for Bridge and Structural Engineering, Zurich, pp. 1057-1064.

Smyth, B., Keane, M. T. (1995): “Remembering To Forget”, *Proceedings of the 14th International Joint Conference in Artificial Intelligence*, Montreal, Canada, Morgan Kaufmann, San Mateo, pp. 377-382.

SNNS (2001). “Stuttgart Neural Net Simulator”, http://www-ra.informatik.uni-tuebingen.de/SNNS/, last visited May 2002.

Szilard, R. (1982). “Finite Berechnungsmethoden der Strukturmechanik“, *Band 1: Stabwerke*, Ernst & Sohn Verlag, Berlin.

Takenaka (2002). “Cable Structures”, http://www.takenaka.co.jp/takenaka_e/dome_e/history/tech/cable.html: last visited May 2002.

Underwood, P. (1983). “Dynamic Relaxation”, *Computational methods for transient analysis*, Belytschko, T.; Hughes, T.J.R, eds., Elsevier science, pp. 246-265.

Wakefield, D. S. (1999): “Engineering analysis of tension structures: theory and practice”, *Engineering Structures 21*, Elsevier science, pp. 680-690.

Williamson, A., Skelton, R. (1998). “A General Class of Tensegrity Systems”, *Proceedings: Engineering Mechanics for the 21st Century*, ASCE Conference, La Jolla, California, May 17-20, pp. 1-7.

Zagar, Z., Delic, D. (1993). “Intelligent computer integrated structures: A new generation of structures”, *Advanced Technologies*, Elsevier science, pp. 371-378.

Tables

TABLE 1. Magnitudes and location of the loading

Type	Joint loaded	Prestress [mm]	Loads applied [N]
Symmetric	6, 52, 62	2	152, 388, 623, 860
	5, 48, 61	2	152, 388, 623, 860
Asymmetric	6	2	152, 388, 623, 860
	52	2	152, 388, 623, 860
	62	2	152, 388, 623, 860
	5	2	152, 388, 623, 860
	48	2	152, 388, 623, 860
	61	2	152, 388, 623, 860
Central joint	7	2	152, 388, 623, 860, 981, 1216, 1452, 1687, 1923
	54	2	152, 388, 623, 860, 981, 1216, 1452, 1687, 1923
	63	2	152, 388, 623, 860, 981, 1216, 1452, 1687, 1923
	7	3	388, 860, 1216, 1687
	54	3	388, 860, 1216, 1687
	63	3	388, 860, 1216, 1687
	7	4	388, 860, 1216, 1687
	54	4	388, 860, 1216, 1687
	63	4	388, 860, 1216, 1687
	7, 54, 63	2	152, 388, 623, 860, 981, 1216, 1452

TABLE 2. Comparison of four network topologies. The two best networks (3-12-3 and 3-14-14-3) are studied further in Figure 9.

Network	Test Error (SSE)
3-8-3	8.10E-02
3-12-3	7.98E-02*
3-10-10-3	8.09E-02
3-14-14-3	7.87E-02*

*used for evaluation with unseen data

TABLE 3. Comparison of four network topologies, trained with the average of data triples

Network	Test Error (SSE)
3-8-3	5.80E-03
3-12-3	6.05E-03
3-10-10-3	5.24E-03
3-14-14-3	5.79E-03

Figures

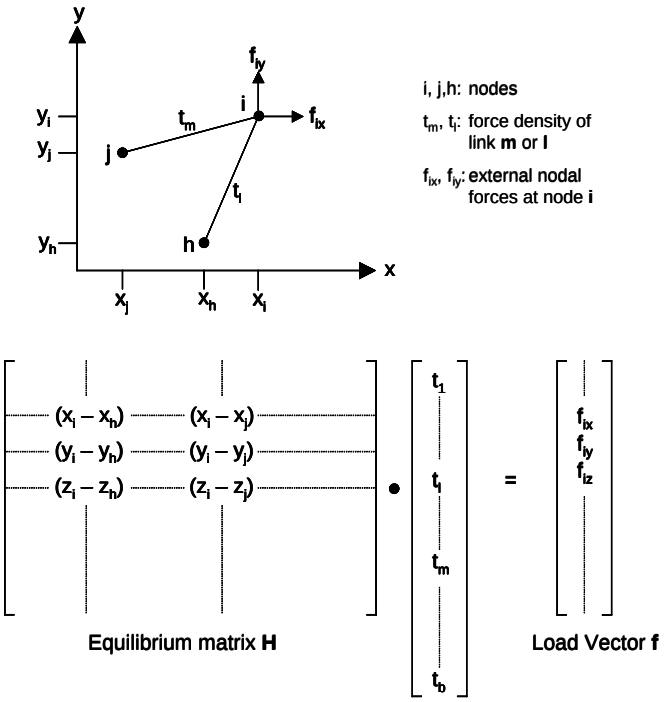

FIG. 1. Expressing the equilibrium of a structure in matrix form, as presented in Pellegrino and Calladine 1986

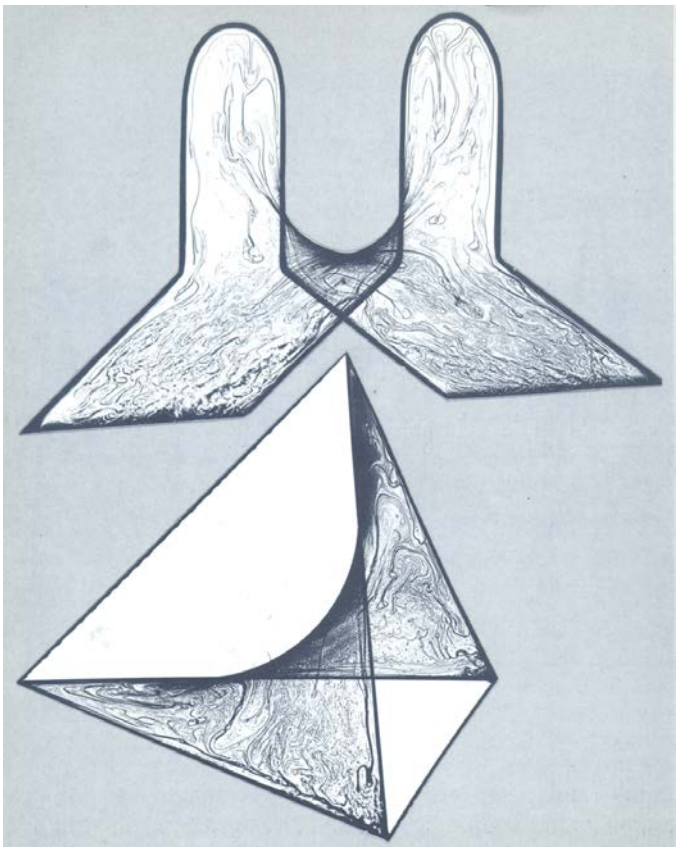

FIG. 2. Form finding with soap films (Bach 1998)

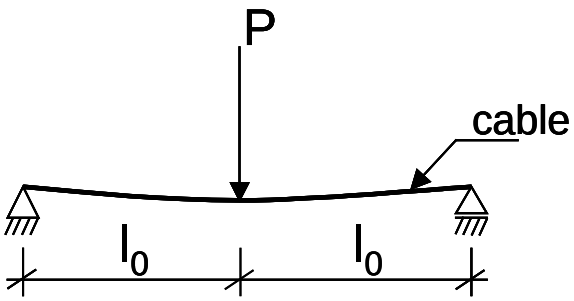

FIG. 3. Cable between two supports

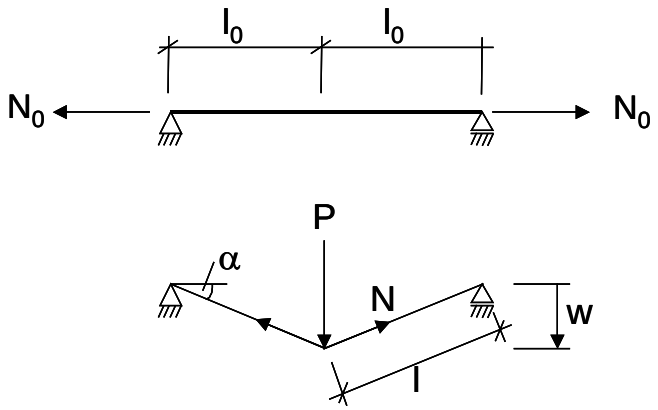

FIG. 4. Cable between two supports: deformed state

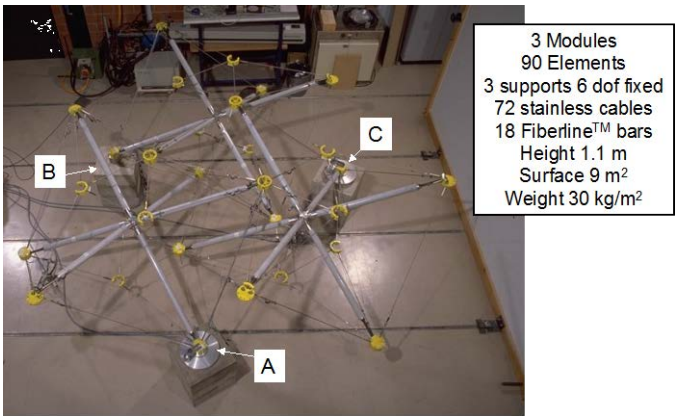

FIG. 5. Photo of tensegrity structure (A, B and C are supports)

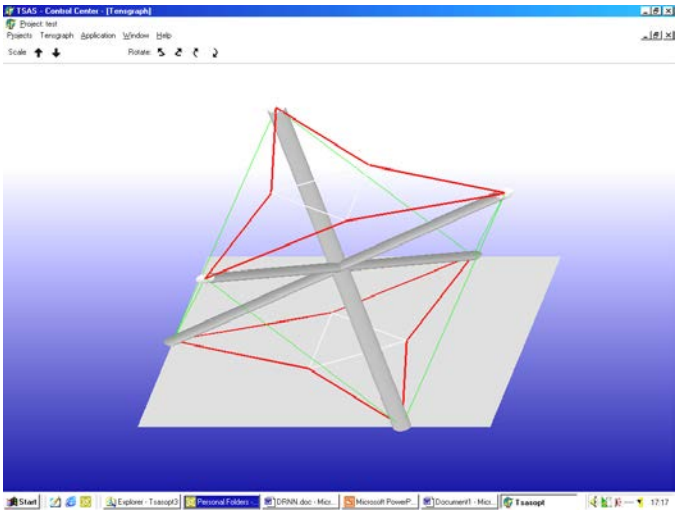

FIG. 6. One module (screen shot from TSCACS)

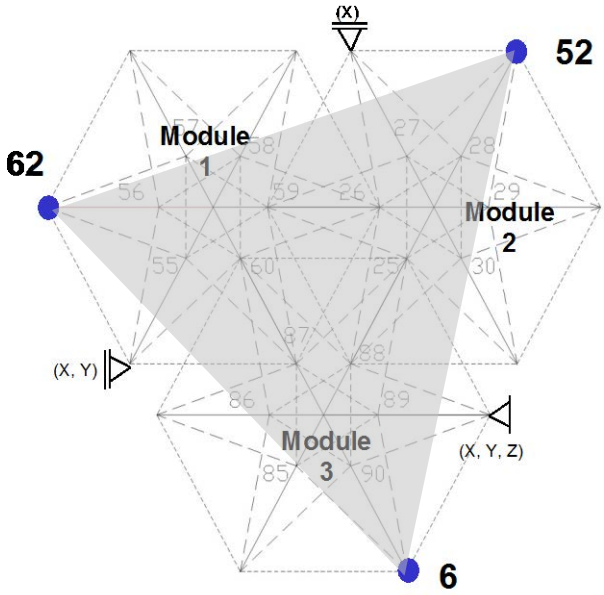

FIG. 7. The control objective involved maintaining the slope constant between nodes 6, 52 and 62.

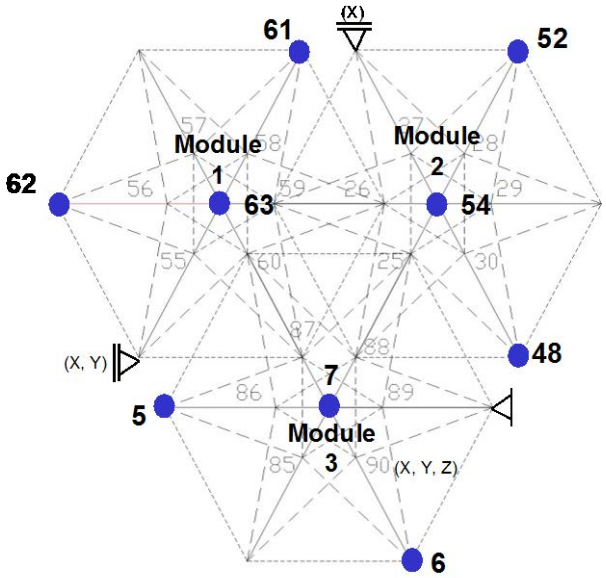

FIG. 8. Node numbers of loaded joints, corresponding to Table 1

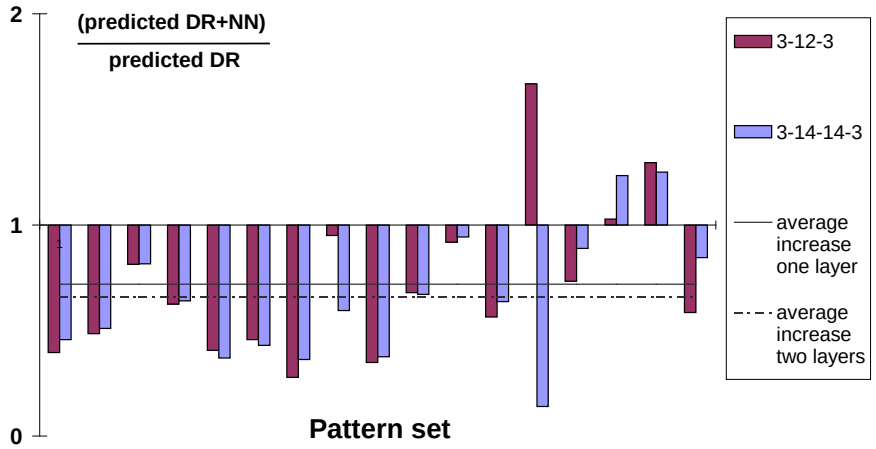

FIG. 9. Accuracy loss for the 3-12-3 and the 3-14-14-3 topology

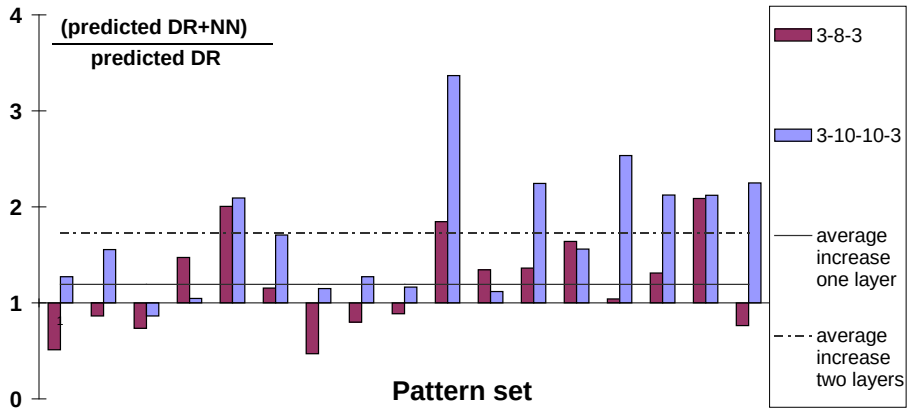

FIG. 10. Accuracy enhancement for the 3-8-3 and the 3-10-10-3 topology

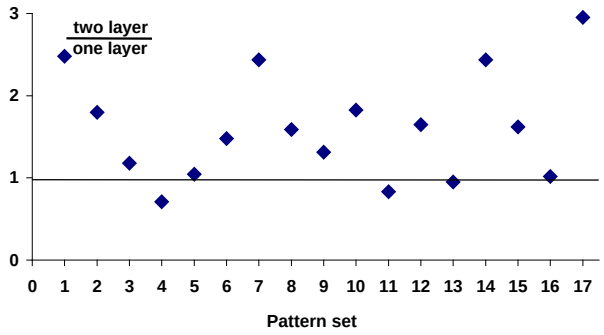

FIG. 11. Comparison of the two layer/one layer configuration

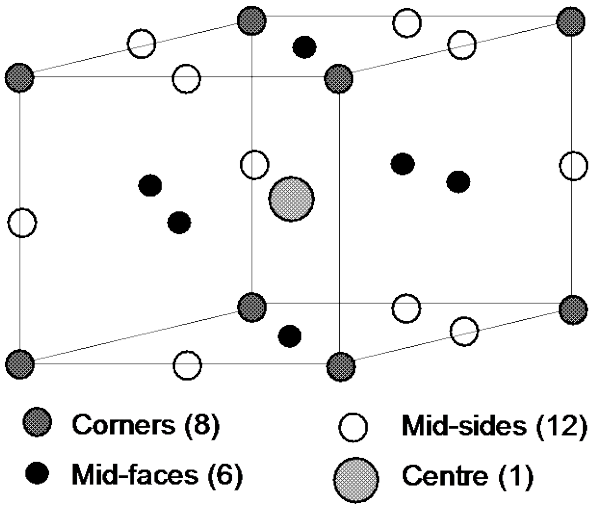

FIG. 12. Hypercube (as presented in Rafiq, Bugman and Easterbrook 2000)

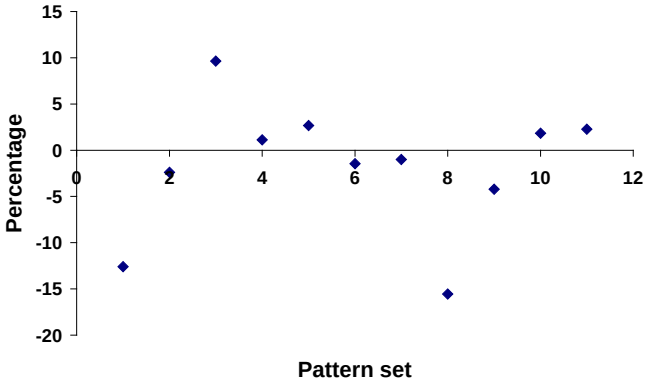

FIG. 13. Percentage deviations for the test patterns (3-8-8-1 network, sigmoid activation function)

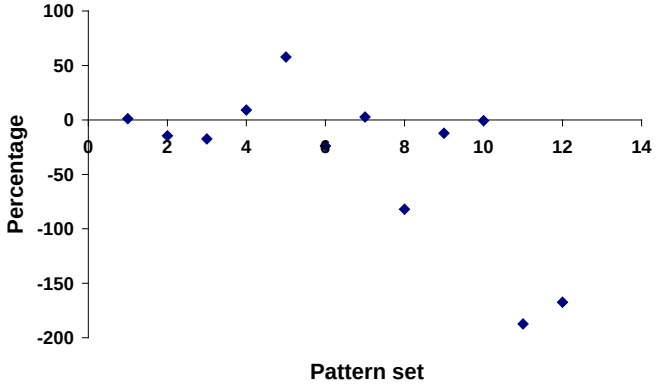

FIG. 14. Percentage deviations for the test patterns (3-8-8-1 network, tanh activation function)

List of figure captions